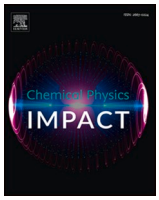
Chemical Physics Impact 9 (2024) 100776



Contents lists available at ScienceDirect

Chemical Physics Impact

journal homepage: www.sciencedirect.com/journal/chemical-physics-impact



Effect of ordering of B' site atom on the dynamical lattice properties of sustainable $Sr_2B'WO_6$ (B'= Co, Ni) double Perovskite

Neetu Malik [a,b], Ruby Jindal [a,*], Archana Tripathi [c], Neeraj Kumari [a]

[a] School of Basic & Applied Sciences, K.R. Mangalam University, Gurugram, Haryana 122103, India
[b] Department of Chemistry, Pt. Jawaharlal Nehru Govt. College, Faridabad, Haryana121002, India
[c] Department of Physics, Deshbandhu College (University of Delhi), New Delhi 110019, India

ARTICLE INFO

Keywords:
Group D elements
Sustainable double Perovskites
Phonon
Raman wavenumber
Infrared wavenumbers
Magnetic material

ABSTRACT

The wavenumbers of Raman and infrared spectra for environment friendly double perovskite $Sr_2B'WO_6$ (B'= Co, Ni) of I4/m phase (No.-87) has been analyzed using Wilson's GF matrix method. Theoretical assignments for the Raman and infrared wavenumbers for Sr_2CoWO_6 and Sr_2NiWO_6 compounds have been reported for the very first time. As far as we know, no theoretical assignments have been made for the infrared frequencies of Sr_2CoWO_6 and Sr_2NiWO_6 compounds in the I4/m phase. Both compounds are Lead-free oxide double perovskites which are emerging as a sustainable alternative to lead-based versions, offering similar electronic, optical, and magnetic properties without the associated environmental and health risks. A robust correlation with the B' site has been identified across a range of frequencies, providing insights into the structural details of the examined compounds. The force constants related to the B'-site atom exhibit a consistent trend and reveal variations in values with changes in atomic orbitals. Moreover, frequencies influenced primarily by the B' atoms display distinct characteristics with the variation of atomic number, emphasizing the considerable effect of the B' atom's size on vibrational properties. The frequencies determined in this research align well with experimentally observed frequencies. Additionally, an exploration of potential energy distributions (PED) delves into the influence of interatomic forces on the computed Raman and infrared phonon modes for these materials.

1. Introduction

In recent times, oxide double perovskites have drawn considerable attention due to their remarkable magnetic properties, including paramagnetism, ferromagnetism, and magnetoresistance capabilities [1–5]. In double perovskites, lead often serves as a key component in the crystal structure, particularly in lead-halide double perovskites like lead-based oxides or halides. The presence of lead contributes to the unique optical and electronic properties of these materials, making them useful in various applications, such as photovoltaics, light-emitting devices, and sensors. But, Lead-based double perovskites pose significant environmental hazards due to the toxicity and persistence of lead. One of the primary concerns is lead toxicity, which can cause severe health issues in humans, animals, and plants, including neurological damage and organ failure. Additionally, these materials can contaminate soil and water, leading to widespread environmental pollution that affects ecosystems, food safety, and water supplies. Another risk is bioaccumulation, where lead accumulates in living organisms and enters the food chain, posing long-term health risks even at low exposure levels. Disposal of lead-based materials also presents challenges, as improper handling can release harmful pollutants into the environment, necessitating strict regulations and management practices. These concerns emphasize the importance of developing lead-free alternatives or implementing safer disposal methods to minimize environmental impact.

Double perovskite compounds can be derived from the simple perovskite structure with the general formula ABO_3, renowned for showcasing a diverse array of compelling properties. The perovskite structure, known for its structural and compositional flexibility, allows for the incorporation of nearly all elements from the periodic table [6]. Double perovskites are compounds characterized by the general formula $A_2B'B''O_6$, representing an advanced version of simple perovskites wherein the unit cell in double perovskites is twice that of their simpler counterparts. Within the double perovskite structure, the A site typically accommodates alkaline earth metals or lanthanides, while B′ and B″ usually consist of transition metals [7]. The crystal lattice of double perovskites can be elucidated as a three-dimensional arrangement of

* Corresponding author.
E-mail address: ruby.jindal@krmangalam.edu.in (R. Jindal).

https://doi.org/10.1016/j.chphi.2024.100776
Received 9 October 2024; Received in revised form 10 November 2024; Accepted 11 November 2024
Available online 13 November 2024
2667-0224/© 2024 The Author(s). Published by Elsevier B.V. This is an open access article under the CC BY-NC-ND license (http://creativecommons.org/licenses/by-nc-nd/4.0/).

corner-sharing octahedra. In this configuration, the larger A-sites are occupied by A cations, while the smaller B-sites are populated by B and B' cations, with oxygen atoms positioned at the octahedra centers. This arrangement results in a cubic crystal structure with a perovskite lattice [6,8,9].

A-site cations are commonly selected from alkaline earth metals like strontium (Sr), calcium (Ca) or barium (Ba). B and B' cations can be a combination of transition metals or rare earth elements [8]. The specific properties of the double perovskite, encompassing magnetic, electronic, dielectric [10–12] and optical characteristics, are determined by the choice of these cations. Group D elements (transition metals) play a fundamental role in determining the structural, electronic, optical, magnetic, and catalytic features of double perovskites. By carefully selecting and tuning these elements, researchers can design materials with tailored properties for specific technological applications, from renewable energy to advanced electronic devices. The ongoing research in this field aims to uncover new combinations and understand the fundamental mechanisms driving the exceptional properties of these fascinating materials [6,13]. The d-orbitals of transition metals significantly affect the electronic band structure of double perovskites. This can result in Semiconducting behavior, metallic and half-metallic properties and magnetic ordering [1,14]. Transition metals can influence the optical absorption and emission properties of double perovskites. For instance, the presence of transition metals can shift the absorption edge and alter the material's color, impacting its suitability for light-harvesting applications. Some transition metal-doped perovskites show strong luminescence, which is beneficial for optoelectronic applications like LEDs and lasers.

Additionally, their structural flexibility allows for the substitution of different cations and the fine-tuning of lattice parameters, influencing the stability and performance of the material across various applications. Some double perovskites may also display catalytic activity, making them relevant for applications in catalysis and chemical processes. In the realm of photovoltaics, double perovskites have gained recognition for their ability in creating efficient and stable solar cells, thanks to their tunable bandgaps and optoelectronic properties. Furthermore, certain double perovskites may exhibit ion conductivity, a valuable feature for applications in solid oxide fuel cells and other electrochemical devices [15–22].

2. Structure

At room temperature and pressure, the $Sr_2B'WO_6$ (B'= Co,Ni) ordered double perovskite tungstate oxide adopts a tetragonal phase with the space group I4/m (No. 87), as elucidated by studies with the following lattice parameters:

For Co, a, $b = 5.5880$ Å and $c = 7.9470$ Å [23].

For Ni, a, $b = 5.5644$ Å, $c = 7.9025$ Å [24].

Strontium (Sr), oxygen O_1 and oxygen O_2 atoms are positioned at 4d (0.00, 0.50, 0.25), 8 h (x, y, 0), and 4e (0, 0, z) Wyckoff sites, respectively, while Tungsten (W) together with Copper (Co), Nickel (Ni) atoms are situated at octahedral positions 2b (0, 0, 0.5) and 2a (0, 0, 0), respectively [23].

Total count for zone center phonon modes for the $Sr_2CoB'O_6$ compound within the I4/m space group is

$$\Gamma_{total} = 3A_g + 3B_g + 6E_g + 5A_u + 1B_u + 12E_u$$

Among these 30 modes, 1Au + 2Eu constitute the acoustical modes, while remaining 27 modes are classified as optical-active modes, as described by the following equation.

$$\Gamma optical = 3A_g + 3B_g + 6E_g + 4A_u + 1B_u + 10E_u$$

The Raman modes consist of 3Ag, 3Bg, and 6Eg, whereas the Infrared modes include 10Eu, 4Au and 1Bu. Non-degenerate modes are Bg and Ag, while Eg represents double-degenerate modes. Structure of $Sr_2B'WO_6$ consists of alternating $B'O_6$ and WO_6 octahedra [23,25–27] with Sr atoms surrounded by 12 oxygen anions while, B' and W atoms are surrounded by 6 oxygen anions. Crystal structure of Sr_2CoWO_6 is shown below in Fig. 1.

3. Theory

To ascertain the frequency of normal vibrations, incorporating the kinetic and potential energies of the system, it is crucial to solve the Eigenvalue equation through the application of Wilson's GF matrix method [28]. The corresponding equation of Eigenvalue can be found below

$$det|FG - E\lambda| = 0$$

The force constants matrix F, denoted by K_i and H_i (associated with stretching and bending force constants, respectively), is expressed in terms of potential energies related to vibrations. G represents the inverse kinetic energy matrix involving masses. The Eigenvalues λ represent frequencies and are given by $\lambda = 4\pi^2c^2\nu^2$, where c represents velocity of light and ν represents wavenumber. E denotes the unit matrix [29].

Hooke's law governs the stretching vibrational forces between different atoms. Both stretching forces and bending vibrational forces play a crucial role in computing transverse vibrations within crystal lattice. The variation in a triangle's angle can be determined by comparing the triangle in its equilibrium state using the projection of deformed triangle onto the equilibrium plane [30–31].

The potential energy includes short-range stretching forces (W-O1, W-O2, B'-O1, B'-O2, Sr-O1, Sr-O2) and bending forces (O1-Sr-O2, B'-O1-W). The input parameters include lattice dimensions, atomic masses, and symmetry coordinates employed in the measurement. The force constants associated with short-range interactions, specifically for bond stretching and angle bending, are refined and optimized to align the calculated Raman and infrared wavenumbers with experimental values. Atomic coordinate, Wyckoff sites and phonons for the double perovskite oxide compound $Sr_2B'WO_6$ (B'= Co, Ni) with the I4/m space group, are presented in below (Table 1).

4. Results and discussion

In this study, we have calculated the zone center Raman and IR phonons for tetragonal double perovskite $Sr_2B'WO_6$ (B' = Co, Ni) compounds in the I4/m phase, using nine short-range force constants (both stretching and bending), as detailed in Table 2.

As depicted from table above; for B'-O2 and B'-O1 (B' = Co, Ni) bonds, the force constant remains almost same. As atomic mass of Co and Ni is almost same, so no appreciable change in force constants is observed for these bonds. Tetragonal Sr_2 $NiWO_6$ features NiO_6 and WO_6 octahedra, which vary in their bond lengths. The equatorial bond lengths in NiO_6 are significantly shorter than those in WO_6, whereas the apical bond lengths in NiO_6 are slightly longer than those in WO_6. [24]. As a result, the W-O2 bond length is shorter than the W-O1 bond length in Sr_2 $NiWO_6$, whereas in Sr_2 $CoWO_6$, the W-O1 bond length is shorter than the W-O2 bond length. Consequently, the force constant of the W-O1 bond decreases when moving from Co to Ni, while that of the W-O2 bond increases. For Sr-O2 and Sr-O1 bonds force constant remains almost constant as bond length is nearly same.

The vibrational modes as observed in Raman and infrared (IR) spectroscopy of the compounds $Sr_2B'WO_6$ (B' = Co, Ni) have been calculated at the zone center using short-range force constants (K and H), with the results shown in Table 2. $Sr_2B'WO_6$ (B' = Co, Ni) are isostructural compounds from the same family of d-block elements, differing only in the atomic number of the B' atom. To our knowledge, there has been no prior theoretical research and experimental research is also limited on the Raman and IR vibrational modes for Sr_2CoWO_6 and Sr_2NiWO_6 compounds. This study provides the first theoretical assignments of these modes for Sr_2CoWO_6 and Sr_2NiWO_6. We recognize the

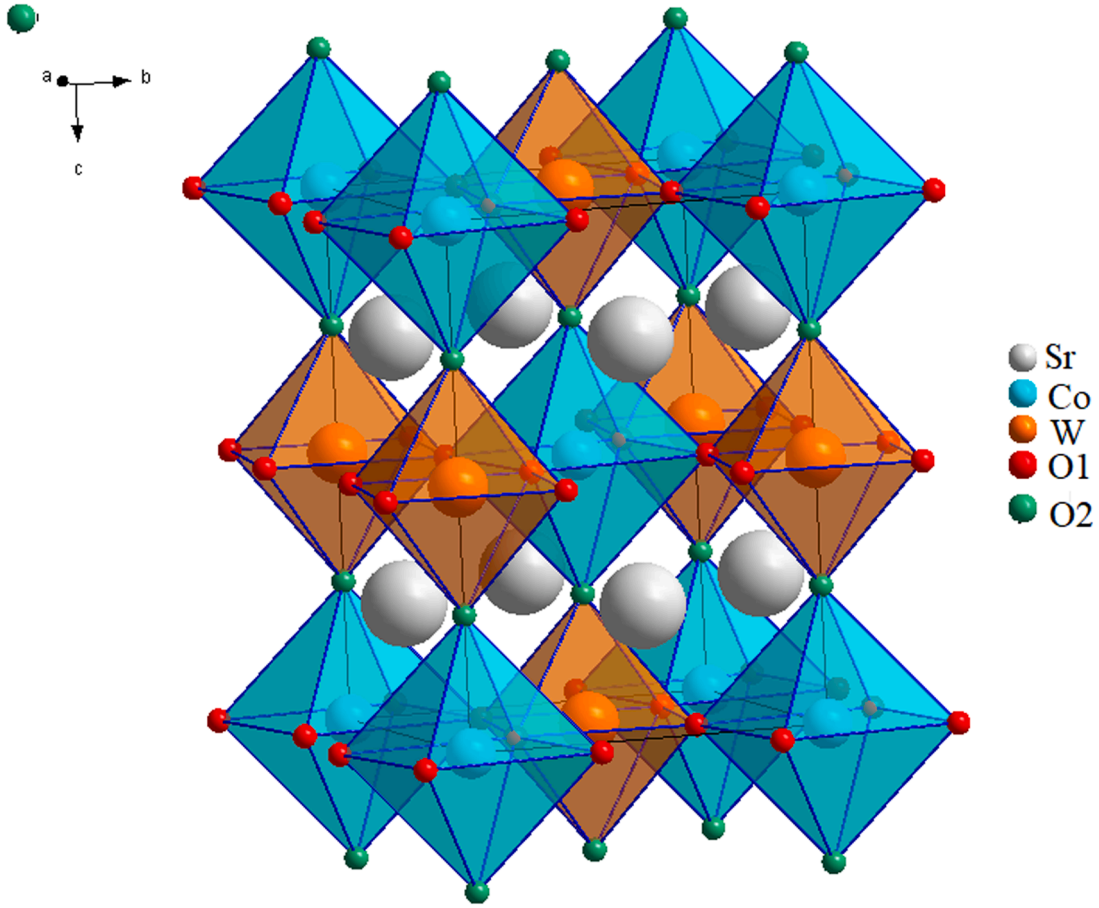


Fig. 1. Crystal structure of Sr_2CoWO_6.

Table 1
Atomic coordinate, Wyckoff Sites, and the phonon contribution for $Sr_2B'WO_6$ (B'= Co,Ni) at Γ point [23].

Atoms	Wyckoff sites	x		y		z		Phonon contribution
		Co	Ni	Co	Ni	Co	Ni	
Sr	4d	0.0000	0.0000	0.5000	0.5000	0.2500	0.2500	Bg + Eg + Au + Eu
B'	2a	0.0000	0.0000	0.0000	0.0000	0.0000	0.0000	Au + Eu
W	2b	0.0000	0.0000	0.0000	0.0000	0.5000	0.5000	Au + Eu
O1	8h	0.2911	0.2690	0.2250	0.2000	0.0000	0.0000	2Ag + 2Bg + Eg + Au +2Eu+ Bu
O2	4e	0.0000	0.0000	0.0000	0.0000	0.2598	0.2550	Ag + Eg + Au +Eu

Table 2
Interatomic Force Constant (FC) Values (in 10^2 N/m) with Coordination Number (CN) for $Sr_2B'WO_6$ (B'= Co,Ni) compounds in I4/m structure.

Sr_2CoWO_6					Sr_2NiWO_6				
F C	Between atoms	CN	Distance (å) /angles (°)	FC value (N/cm)	FC	Between atoms	CN	Distance (å) /angles (°)	FC value (N/cm)
K_1	Co-O2	2	1.9089	1.459	K_1	Ni-O1	4	1.8652	2.005
K_2	W-O1	4	1.9298	1.390	K_2	Ni-O2	2	1.9361	1.509
K_3	Co-O1	4	2.0559	1.323	K_3	W-O2	2	2.0151	1.449
K_4	W-O2	2	2.0646	1.211	K_4	W-O1	4	2.1069	0.666
K_5	Sr-O1	8	2.6250	0.097	K_5	Sr-O1	8	2.6065	0.094
K_6	Sr-O2	8	2.7951	0.081	K_6	Sr-O2	8	2.7825	0.074
H_1	O1-Sr-O2	8	121.660	1.001	H_1	O1-Sr-O2	8	119.436	0.963
H_2	O1-Sr-O2	8	122.129	0.117	H_2	O1-Sr-O2	8	124.607	0.022
H_3	O1-Co-W	4	164.923	0.052	H_3	O1-Ni-W	4	164.227	0.048

significance of experimental IR and Raman spectra in validating theoretical predictions and enriching the overall impact of the research. As theorists, we are aware of the limited availability of experimental data in the literature. Our theoretical investigation of these compounds is intended to motivate experimentalists to undertake the necessary experimental work to complement our results. The theoretical outcomes for Raman and Infrared wavenumbers are then juxtaposed with the Raman and infrared wavenumbers experimentally determined by Ayala et al. [26] and Manoun et al. [32] as presented in Table 3. The comparison strongly reinforces the conclusion that the calculated results are

Table 3
Presently computed Raman and IR zone-center vibrational modes, along with experimentally determined modes (in cm^{-1}) for the $Sr_2B'WO_6$ (B'= Co, Ni) compound.

Species	Observed Wave numbers by Ayala for Sr_2CoWO_6 (in cm-1)	Observed wavenumbers by Igartua for Sr_2CoWO_6 (in cm-1)	Presently calculated wave numbers for Sr_2CoWO_6 (in cm-1)	Presently calculated wave numbers for Sr_2NiWO_6 (in cm-1)
A_{g1}	850	864	853.1	853.9
A_{g2}	533	572	532	538.1
A_{g3}		225	216.2	215.4
B_{g1}	579	716	690.4	679.0
B_{g2}	303		313.7	316.9
B_{g3}	138	134	182.8	173.5
E_{g1}	443	312	434.1	431.6
E_{g2}			140.5	135.6
E_{g3}			89.6	91.0
A_{u1}			833.3	840.3
A_{u2}			345.6	347.6
A_{u3}			207.0	221.3
A_{u4}			73.3	72.8
B_u			226.0	220.8
E_{u1}			719.4	726.6
E_{u2}			374.3	412.6
E_{u3}			246.7	193.0
E_{u4}			163.9	154.9
E_{u5}			79.2	78.5

in conjunction with the Raman and infrared phonon modes that were observed experimentally.

To understand the influence of various force constants to different frequencies, potential energy distributions (PED) for each mode were assessed. Further details on these PED interpretations are provided below.

The observed Raman modes can be categorized into three main groups of lattice vibrations: Sr^{+2} translations, along with the translational and rotational modes of the WO_6 octahedra, occurring at frequencies below 200 cm^{-1}; O–W–O bending vibrations, which are found in the 200–500 cm^{-1} range; and W–O stretching modes, present at frequencies above 500 cm^{-1} [31].

As shown in Table 4, the higher frequency modes of 853.1 cm^{-1} of Ag, 833.3 cm^{-1} of Au, 345.6 cm^{-1} of Au are influenced by the bending vibrations of the O1-Sr-O2 bond and stretching vibrations of B'-O2 bond in both compounds and are accredited by vibrations of apical O2 in B'-O6 octahedra. 719.4 cm^{-1} of Eu, 690.4 cm^{-1} of Bg and 374.3 cm^{-1} of Eu. Modes 532 cm^{-1} of Ag, 246.7 cm^{-1} of Eu are contributed by force constants W-O1 and B'-O1 and are impacted by vibrations of equatorial O1 in B'-O6 octahedra. Force constants O1-Sr-O2 and Sr-O2 attributed to modes 434.1 cm^{-1} of Eg and 79.2 cm^{-1} of Eu; mainly governed by vibrations of O2 Atom. 313.7 cm^{-1} of Bg is governed by vibrations of O1-Sr-O2 and W-O1. 226 cm^{-1} of Bu is governed by vibration of O1-Sr-O2 and Sr-O1. Force Constants Sr-O1 and O1-Co-W are responsible for modes 216.2 cm^{-1} of Ag 182.8 cm^{-1} of Bg, 163.9 cm^{-1} of Eu; mainly governed by O1 atom. 140.5 cm^{-1} of Eg is attributed by vibration of Sr-O1 and Sr-O2. Force constants Sr-O1 and O1-Sr-O2 contributed to mode 89.6 cm^{-1} of Eg and Force constants W-O2 and Sr-O1 contributed to mode 73.3 cm^{-1} of Au.

As concluded form PED, vibrations of apical O2 atom in $B'O_6$ octahedra are responsible for higher frequencies and vibrations of equatorial O1 atom of $B'O_6$ and WO_6 octahedra are responsible for lower wavenumbers.

5. Conclusion

The investigation involves examining the normal coordinates of $Sr_2B'WO_6$ (B'= Co, Ni) Double Perovskite oxides, taking into account six stretching and three bending force constants to evaluate the Raman and infrared phonon modes. To the best of our knowledge, there are no existing theoretical calculations for Raman and Infrared wavenumbers concerning $Sr_2B'WO_6$ (B'= Co, Ni) oxides, which are lead free and hence emerge as sustainable alternative to lead based versions. This study attempts to comprehensively present all theoretically computed Raman and infrared phonons for the $Sr_2B'WO_6$ (B'= Co, Ni) compounds, including mode assignments. Utilizing the normal coordinate analysis method, we conducted this research. Additionally, we explored potential energy distribution (PED) to analyze the influence of interatomic forces on the computed Raman and infrared phonons.

Table 4
Two Dominant Contributions of Force Constants as per the Potential Energy Distribution (PED) for the $Sr_2B'WO_6$ (B'= Co, Ni) compounds.

Species	Calculated wavenumbers for Sr_2CoWO_6	Two dominant contributions of Force constants as per PED			
		Sr_2CoWO_6		Sr_2NiWO_6	
A_{g1}	853.1	H1=61 %	K1=14 %	H2=58 %	K2=15 %
A_{g2}	532	K2=35 %	K3=33 %	K1=53 %	K4=17 %
A_{g3}	216.2	H3=45 %	K5=18 %	H3=42 %	K5=18 %
B_{g1}	690.4	K3=26 %	H1=50 %	H2=48 %	K1=38 %
B_{g2}	313.7	K2=31 %	H1=44 %	H2=45 %	K1=38 %
B_{g3}	182.8	K5=39 %	H3=46 %	H3=45 %	K5=41 %
E_{g1}	434.1	H1=95 %	K6=3 %	H2=95 %	K6=2 %
E_{g2}	140.5	K6=70 %	K5=28 %	K6=68 %	K5=30 %
E_{g3}	89.6	K5=55 %	H2=26 %	K5=50 %	H1=32 %
A_{u1}	833.3	H1=59 %	K1=24 %	H2=54 %	K2=25 %
A_{u2}	345.6	K1=54 %	H1=33 %	K2=51 %	H2=36 %
A_{u3}	207.0	K4=72 %	K1=21 %	K3=69 %	K2=24 %
A_{u4}	73.3	K5=88 %	K4=6 %	K5=90 %	H2=5 %
B_u	226.0	H1=76 %	K5=23 %	H2=755	K5=23 %
E_{u1}	719.4	H1=46 %	K3=30 %	K1=48 %	H2=39 %
E_{u2}	374.3	H1=45 %	K3=26 %	H2=50 %	K1=41 %
E_{u3}	246.7	K2=46 %	K3=36 %	K4=45 %	H3=23 %
E_{u4}	163.9	H3=45 %	K5=20 %	H3=37 %	K4=33 %
E_{u5}	79.2	K6=46 %	H2=18 %	K6=45 %	H3=13 %

CRediT authorship contribution statement

Neetu Malik: Writing – original draft, Visualization, Validation, Supervision, Software, Resources, Methodology, Investigation, Formal analysis, Data curation, Conceptualization. **Ruby Jindal:** Writing – review & editing, Visualization, Validation, Supervision, Software, Resources, Methodology, Investigation, Formal analysis, Data curation, Conceptualization. **Archana Tripathi:** Writing – review & editing, Visualization, Validation, Software, Resources, Methodology, Formal analysis, Conceptualization. **Neeraj Kumari:** Visualization, Validation, Formal analysis, Data curation, Conceptualization.

Declaration of competing interest

The authors declare that they have no known competing financial

interests or personal relationships that could have appeared to influence the work reported in this paper.

Data availability

Data will be made available on request.

References

[1] D.D. Sarma, P. Mahadevan, T. Saha-Dasgupta, S. Ray, A. Kumar, Electronic Structure of Sr 2 FeMoO 6, Phys. Rev. Lett. 85 (12) (2000 Sep 18) 2549–2552.

[2] Z. A, D.J. J.w, F. R, T.N. L, Z. A, D.J. J.w, et al., Preparation, crystal and magnetic structure of the double perovskite Ba2FeWO6, Appl Phys Mater Sci Process 74 (1 Suppl) (2002 Jan 1) S763–S765.

[3] R.N. Mahato, K. Sethupathi, V. Sankaranarayanan, Colossal magnetoresistance in the double perovskite oxide La2CoMnO6, J. Appl. Phys. 107 (9) (2010 Apr 19) 09D714.

[4] S. Sengodan, S. Choi, A. Jun, T.H. Shin, Y.W. Ju, H.Y. Jeong, et al., Layered oxygen-deficient double perovskite as an efficient and stable anode for direct hydrocarbon solid oxide fuel cells, Nat. Mater. 14 (2) (2015 Feb) 205–209.

[5] K.I. Kobayashi, T. Kimura, H. Sawada, K. Terakura, Y. Tokura, Room-temperature magnetoresistance in an oxide material with an ordered double-perovskite structure, Nature 395 (1998 Oct 1) 677–680.

[6] T. Saha-Dasgupta, Double perovskites with 3d and 4d/5d transition metals: compounds with promises, Mater. Res. Express. 7 (1) (2020 Jan) 014003.

[7] A. Smerechuk, R. Morrow, S. Wurmehl, O. Sidletskiy, Synthesis of magnetically frustrated oxides with double perovskite structure, Acta Crystallogr Sect Found Adv 77 (a2) (2021 Aug 14) C428. –C428.

[8] S. Vasala, M. Karppinen, A2B′B″O6 perovskites: A review, Prog Solid State Chem 43 (1) (2015 May 1) 1–36.

[9] G. King, P.M. Woodward, Cation ordering in perovskites, J. Mater. Chem. 20 (28) (2010 Jul 6) 5785–5796.

[10] X. Wang, T. Liu, Z. Cao, Z. Li, Y. Xu, F. Shi, et al., Lattice vibrational characteristics and structure-property relationships of Ca (Mg1/2W1/2)O3 microwave dielectric ceramics with different sintering temperatures, Ceram. Int. 48 (1) (2022 Jan 1) 1415–1422.

[11] X. Wang, J. Lv, Y. Xu, L. Zhang, Y. Shen, H. Zhou, et al., Dielectric responses and structure-property relationships of Ca1-xBaxWO4 composite microwave dielectric ceramics, J. Alloys. Compd. 925 (2022 Dec 5) 166669.

[12] Z. An, J. Lv, X. Wang, Y. Xu, L. Zhang, F. Shi, et al., Effects of LiF additive on crystal structures, lattice vibrational characteristics and dielectric properties of CaWO4 microwave dielectric ceramics for LTCC applications, Ceram. Int. 48 (20) (2022 Oct 15) 29929–29937.

[13] D.D. Sarma, P. Mahadevan, T. Saha-Dasgupta, S. Ray, A. Kumar, Electronic Structure of ${\mathrm{Sr}}_{2}{\mathrm{FeMoO}}_{6}$, Phys. Rev. Lett. 85 (12) (2000 Sep 18) 2549–2552.

[14] H. Das, U.V. Waghmare, T. Saha-Dasgupta, D.D. Sarma, Electronic Structure, Phonons, and Dielectric Anomaly in Ferromagnetic Insulating Double Pervoskite La 2 NiMnO 6, Phys. Rev. Lett. 100 (18) (2008 May 5) 186402.

[15] H. Benmhidi, H. Rached, D. Rached, M. Benkabou, Ab Initio Study of Electronic Structure, Elastic and Transport Properties of Fluoroperovskite LiBeF3, J. Electron. Mater. 46 (4) (2017 Apr 1) 2205–2210.

[16] Bourachid I., Caid Caid M., Cheref O., Rached D., Heireche H., Abidri B., et al. Insight into the structural, electronic, mechanical and optical properties of inorganic lead bromide perovskite APbBr3 (A = Li, Na, K, Rb, and Cs). 2020 May 1; 24:e00478.

[17] A. Candan, M. Kurban, Electronic structure, elastic and phonon properties of perovskite-type hydrides MgXH3 (X = Fe, Co) for hydrogen storage, Solid. State Commun. 281 (2018 Oct 1) 38–43.

[18] S. Al-Qaisi, M. Mushtaq, S. Alomairy, T. Vu, H. RACHED, B. Ul Haq, et al., First-principles investigations of Na2CuMCl6 (M = Bi, Sb) double perovskite semiconductors: Materials for green technology, Mater. Sci. Semicond. Process. 150 (2022 Jul 11).

[19] F. Igbari, Z.K. Wang, L.S. Liao, Progress of Lead-Free Halide Double Perovskites, Adv. Energy Mater. 9 (2019 Feb 1).

[20] U. Rani, P. Kamlesh, R. Agrawal, A. Shukla, A. Verma, Emerging Study on Lead-Free Hybrid Double Perovskite (CH3NH3)2AgInBr6: Potential Material for Energy Conversion between Heat and Electricity, Energy Technol 10 (2022 Jul 20).

[21] Y. Soni, U. Rani, A. Shukla, T. Joshi, A. Verma, Transition metal-based halides double Cs2ZSbX6 (Z = Ag, Cu, and X = Cl, Br, I) perovskites: A mechanically stable and highly absorptive materials for photovoltaic devices, J. Solid. State Chem. 314 (2022 Jul 1) 123420.

[22] X. Zhao, L. Zhang, Z. Xiao, Y Sun, Rational Design of Halide Double Perovskites for Optoelectronic Applications, Joule 2 (2018 Sep 19).

[23] M. Dhilip, M. Marimuthu, R. Sundaramurthy, V. Jayalakshmi, A. Venugopalan, S. Krishnaswamy, Synthesis of SrCoO3 perovskite as W-based double perovskite and its structural properties, J Mater Sci Mater Electron 30 (2019 Feb 1).

[24] J. Bijelić, D. Tatar, S. Hajra, M. Sahu, S.J. Kim, Z. Jagličić, et al., Nanocrystalline Antiferromagnetic High-κ Dielectric Sr2NiMO6 (M = Te, W) with Double Perovskite Structure Type, Molecules. 25 (17) (2020 Jan) 3996.

[25] M. Viola, M. Martínez-Lope, J. Alonso, J. Martínez, J. De Paoli, S. Pagola, et al., Structure and Magnetic Properties of Sr2CoWO6: An Ordered Double Perovskite Containing Co2+ (HS) with Unquenched Orbital Magnetic Moment, Cheminform 34 (2003 Apr 1).

[26] A.P. Ayala, Raman investigation of A2CoBO6 (A=Sr and Ca, B=Te and W) double perovskites, J. Appl. Phys. 101 (12) (2007) 123511.

[27] N. Saadon, N. Ali, N. Ibrahim, Z Mohamed, Structural and optical properties of Sr2NiWO6 double perovskite, in: AIP Conference Proceedings 2368, 2021 030006.

[28] T. Shimanouchi, M. Tsuboi, T. Miyazawa, Optically Active Lattice Vibrations as Treated by the GF-Matrix Method, J. Chem. Phys. 35 (5) (2004 Aug 4) 1597–1612.

[29] R. Jindal, M.M. Sinha, H.C. Gupta, Study of Zone Center Phonons in $CdWO_4$, Int J Eng Res Technol [Internet] 1 (1) (2018 Jul 30) [cited 2023 Dec 25]Available from: https://www.ijert.org/research/study-of-zone-center-phonons-in-cdwo4-IJERTCONV1IS01009.pdf.

[30] R. Jindal, M.M. Sinha, H.C Gupta, Lattice vibrations of AVO4 crystals (A= Lu, Yb, Dy, Tb, Ce), Spectrochim. Acta a Mol. Biomol. Spectrosc. 113 (2013) 286–290.

[31] R. Jindal, M.M. Sinha, Gupta HC Study of Zone Center Phonons in CdWO4, Turkish Journal of Physics 37 (2013) 107–112.

[32] B. Manoun, J.M. Igartua, M. Gateshki, S.K. Saxena, High-pressure study of the Sr2CoWO6 ordered double perovskite tungstate oxide, J. Mol. Struct. 888 (1) (2008 Oct 15) 244–252.